Saturated fatty acids activate microglia via Toll-like receptor 4/NF-κB signalling

Zhen Wang[1], Dexiang Liu[1], Fuwu Wang[1], Shangming Liu[1], Shidou Zhao[1], Eng-Ang Ling[2] and Aijun Hao[1]*

[1]*Shandong Provincial Key Laboratory of Mental Disorders, Department of Histology and Embryology, Shandong University School of Medicine, 44#, Wenhua Xi Road, Jinan, Shandong 250012, People's Repubic of China*
[2]*Department of Anatomy, Yong Loo Lin School of Medicine, National University of Singapore, 4 Medical Drive, MD10, Singapore 117597, Singapore*

Abstract

Diets rich in SFA have been implicated in Alzheimer's disease (AD). There is strong evidence to suggest that microglial activation augments the progression of AD. However, it remains uncertain whether SFA can initiate microglial activation and whether this response can cause neuronal death. Using the BV-2 microglial cell line and primary microglial culture, we showed that palmitic acid (PA) and stearic acid (SA) could activate microglia, as assessed by reactive morphological changes and significantly increased secretion of pro-inflammatory cytokines, NO and reactive oxygen species, which trigger primary neuronal death. In addition, the mRNA level of these pro-inflammatory mediators determined by RT-PCR was also increased by PA and SA. We further investigated the intracellular signalling mechanism underlying the release of pro-inflammatory mediators from PA-activated microglial cells. The present results showed that PA activated the phosphorylation and nuclear translocation of the p65 subunit of NF-κB. Furthermore, pyrrolidine dithiocarbamate, a NF-κB inhibitor, attenuated the production of pro-inflammatory mediators except for IL-6 in PA-stimulated microglia. Administration of anti-Toll-like receptor (TLR)4-neutralising antibody repressed PA-induced NF-κB activation and pro-inflammatory mediator production. In conclusion, the present *in vitro* study demonstrates that SFA could activate microglia and stimulate the TLR4/NF-κB pathway to trigger the production of pro-inflammatory mediators, which may contribute to neuronal death.

Key words: Microglia: SFA: NF-κB: Toll-like receptor 4

Epidemiological data suggest that a diet rich in SFA is considered an increased risk factor for the development of Alzheimer's disease (AD). For example, in a 21-year follow-up study, it was found that abundant SFA intake from milk products and spreads at midlife was associated with poorer global cognitive function and prospective memory[1]. Other studies have demonstrated that a greater intake of saturated fat increased the risk for impaired cognitive function in middle-aged or aged populations[2–4]. This notion has been supported by animal studies. In this connection, it has been reported that rodents fed high levels of SFA also show impaired learning and memory performance and develop AD-like pathophysiological changes in their brains[5,6]. Fatty acids are free to cross the blood–brain barrier[7]. Therefore, brain fatty acid homeostasis may be dependent on their levels in the periphery. It is therefore conceivable that diets rich in SFA may increase brain uptake of intact NEFA from the plasma through the blood–brain barrier[8]. In addition, the fatty acid profile of neurofibrillary tangles in the AD brain is rich in palmitic acid (PA) and stearic acid (SA)[9], and the white matter in the AD brain is characterised by high total fatty acid contents[10].

PA and SA were reported to increase hyperphosphorylation of tau, and up-regulate β-secretase, the rate-limiting enzyme in the production of amyloid β peptides in primary rat cortical neurons[11,12]. These actions were mediated by the above-mentioned two SFA on astrocytes, possibly through enhanced astrocytic synthesis of ceramide[13]. Several fatty acids have been reported to stimulate the aggregation of tau protein and amyloid β *in vitro*[14]. Despite the accumulating data, the basic mechanism behind the causal relationship

---

between SFA and the pathogenesis of AD has not been well established.

It is well documented that microglia, the resident macrophages in the brain, play a central role in mediating chronic inflammatory conditions in AD[15]. In the ramified state, microglia actively survey the microenvironment and ensure normal central nervous system (CNS) activity by secreting neurotrophic factors such as neuronal growth factor. They are activated in response to specific stimuli and produce a host of pro-inflammatory cytokines, chemokines and reactive oxygen species (ROS). Although microglial activation plays an important role in phagocytosis of dead cells in the CNS, microglia cause inflammatory responses leading to neuronal death and brain injury when they are over-activated and dysregulated[16]. Therefore, identification of the regulators involved in the initiation and maintenance of microglial activation may lead to a better understanding of inflammatory processes leading to AD. However, as far as can be ascertained, there is a total lack of information relating to the modulation of microglial activation by SFA. We report here that SFA could activate microglia to a pro-inflammatory state as evidenced by reactive morphological changes and significantly increased secretion of pro-inflammatory cytokines including TNF-α, IL-1β and IL-6, as well as NO and ROS via Toll-like receptor (TLR)4/NF-κB signalling in the microglial cell line, BV-2 cells, and primary cultures of mouse microglia.

Materials and methods

Animals

BALB/c mice were used. All animals were obtained from the Laboratory Animal Centre, Shandong University. All animals were kept under controlled 12 h light–12 h dark conditions, temperature (23°C) and humidity (60%). In the handling and care of all animals, the International Guiding Principles for Animal Research, as stipulated by the WHO (1985) and as adopted by the Laboratory Animal Centre, Shandong University, were followed. During the study, the number of animals used and their suffering were minimised.

Microglial cell culture

BV-2 cells were maintained in Dulbecco's modified Eagle's medium (DMEM; Hyclone Co., Logan, UT, USA) with 10% fetal bovine serum (Hyclone Co.), 2 mM-L-glutamine, penicillin (100 U/ml) and streptomycin (100 μg/ml) (Sigma-Aldrich, St Louis, MO, USA) in a 5% CO_2 incubator. For all experiments, BV-2 cells were used at 75 to 80% confluency. Before the experiment, plated cells were incubated with serum-free DMEM for 1 h. After this, the medium was replaced with serum-free DMEM containing either PA (16:0; SFA) (Sigma-Aldrich), SA (18:0; SFA) (Sigma-Aldrich), lipopolysaccharide (LPS; Sigma-Aldrich), pyrrolidine dithiocarbamate (PDTC; Sigma-Aldrich) or anti-TLR4-neutralising antibody (anti-TLR4 Ab; eBioscience, Inc., San Diego, CA, USA) for the indicated times.

Primary microglia were prepared from the whole brains of mice, aged 1–2 d, as described previously[17]. Briefly, glial cells were cultured for 14 d in DMEM/F12 (Hyclone Co.) supplemented with 10% fetal bovine serum (Hyclone Co.). Then the mixed glial cultures were shaken on an orbital shaker at 250 rpm for 2 h to dislodge microglial cells. The separate microglial cells were plated into twenty-four-well plates at a density of 2×10^5 cells/well. The purity of the microglia cultures was assessed using CD11b Ab and more than 97% of cells were stained positively. Cells were cultured for 7 d before treatment.

Preparation of fatty acid–albumin complexes

PA or SA was solubilised in ethanol at 70°C. Then PA or SA was combined with fatty acid-free and low-endotoxin bovine serum albumin (BSA) at a molar ratio of 10:1 (fatty acid:albumin) in serum-free medium at 50°C for 6 h for a final PA or SA concentration of 25–200 μM as described previously[18]. The fatty acid–albumin complex solution was freshly prepared before each experiment. The final concentration of ethanol was < 0.5%. In most of the experiments, BV-2 cells or primary microglial cells were treated with individual SFA at 25–200 μM concentration, while the controls received BSA and vehicle only.

To evaluate the possible contamination of PA or SA with LPS, the endotoxin content was determined by the chromogenic Limulus amebocyte lysate test, following the manufacturer's instructions (Cambrex Bio Science, Walkersville, MD, USA). The endotoxin content in the 100 μM-PA and 100 μM-SA solution was ≤ 3.45×10^{-3} pg/ml, which is far below the concentration required to induce microglial activation under our assay conditions.

Conditioned medium

To assess bystander neuronal death by factors released by microglial cells following PA treatment, BV-2 cells were seeded in 60 mm culture plates at a density of 3×10^5 cells/plate. After the cells became confluent, they were incubated with serum-free DMEM for 1 h. After this, the medium was replaced by serum-free DMEM containing appropriate fatty acid–albumin complexes for 12 h. Controls received BSA and vehicle only. After 12 h, the medium was changed with fresh serum-free DMEM for 12 h, and then the supernatant fractions were collected, filtered and added onto primary neurons cultured in poly-D-lysine-coated twelve-well plates.

Neuronal culture and apoptosis analysis

Primary cultures of mouse cortical neurons were prepared as previously described[19]. Briefly, cortical neurons were harvested from mice, aged 1–2 d, using the serum-free Neurobasal medium with B27 supplement system (Invitrogen Corp., Carlsbad, CA, USA). Cortical cells were plated at a density of 1.5×10^6 cells per well in poly-D-lysine-coated twelve-well plates and allowed to differentiate for 7 d. At day 7, the mouse neuronal medium was removed and replaced by a conditioned medium from microglial cells. Neurons were incubated with microglia-conditioned medium for 2 d, and

then analysed by Hoechst 33 342 nuclei staining for the detection of morphological features of apoptotic cell death.

Hoechst was added to the culture medium at a final concentration of 10 μg/ml, which was then incubated in the dark at 100 % humidity for 10 min at 37°C. The cells were then examined under a fluorescence microscope. Undamaged cell nuclei were large and diffusely stained whereas apoptotic nuclei showed chromatin that was condensed and fragmented.

ELISA

BV-2 cells (3×10^5 cells per well in a twelve-well plate) were pretreated with different concentrations of PA (0, 25, 50 or 100 μM), LPS or inhibitors at the indicated times. The supernatant fraction of the culture medium from the various treatments was then collected. The levels of cytokines, TNF-α, IL-1β and IL-6 in the culture medium were measured using commercially available ELISA kits (R&D Systems Inc., Minneapolis, MN, USA) according to the manufacturer's instructions. Briefly, serial dilutions of protein standards and samples were added to ninety-six-well ELISA plates, followed by biotinylated anti-TNF-α, IL-1β or IL-6 Ab. After rinsing with wash buffer, the prepared solution of avidin, horseradish peroxidase-conjugated complex was added followed by the addition of substrate solution. The reaction was terminated by the stopping solution. The optical density was detected at 450 nm in a microplate reader (Bio-Rad Laboratories, Hercules, CA, USA). Each sample concentration was calculated from the linear equation derived from the standard curve of known concentrations of the cytokine.

Assay of NO production

BV-2 cells (3×10^5 cells per well in a twelve-well plate), were pretreated with different concentrations of PA (0, 25, 50 or 100 μM), LPS or inhibitors at the indicated times. The supernatant fraction of the culture medium from the various treatments was collected. NO production was assessed by measuring the accumulation of nitrite in the culture medium by the Griess reaction. The culture medium was mixed with an equal volume of Griess reagent (0·1 % N-1-naphthylethylenediamine dihydrochloride and 1 % sulfanilamide in 5 % phosphoric acid; Sigma-Aldrich) in a ninety-six-well plate and incubated at room temperature for 10 min. Absorbance was measured at 550 nm in a microplate reader (Bio-Rad Laboratories). Sodium nitrite, diluted in culture medium at concentrations ranging from 10 to 100 μM, was used to prepare a standard curve.

Reactive oxygen species assay

Intracellular ROS levels were measured by 2′,7′-dichlorodihydrofluorescein diacetate (H2DCFDA) and dihydroethidium (DHE) assays. H2DCFDA or DHE is a membrane-permeable dye that is oxidised by intracellular ROS to the fluorescent product DCF or ethidium, respectively. Briefly, BV-2 cells were stimulated with or without PA, or LPS for 12 or 24 h, and the culture medium was first removed. The cells were washed

three times with PBS, and were incubated with either 10 μM-H2DCFDA or 2 μM-DHE (Molecular Probes, Eugene, OR, USA) for 20 min at 37°C. The cells were then washed three times with PBS and examined with a Nikon TE2000U microscope (Nikon, Tokyo, Japan). The fluorescence was measured at 485 nm for excitation and 530 nm for emission with a fluorescence plate reader (Fluroskan Ascent II; Labsystems, Helsinki, Finland). The increased value compared with control was considered as the increase of intracellular ROS.

Cell viability assay

Cell viability was determined using the 3-[4, 5-dimethylthiazol-2-yl]-2, 5-diphenyltetrazolium bromide (MTT) assay. BV-2 cells were plated into ninety-six-well culture plates at a density of 1×10^4 cells/well with 200 μl culture medium per well in triplicate. When reaching 75 % confluency, the cells were incubated in the absence or presence of PA (25, 50, 100, 200 μM), respectively, for 48 h. Then, 20 μl MTT solution (5 mg/ml; Sigma-Aldrich) were added to each well and incubated at 37°C for 4 h. The culture medium was aspirated and followed by the addition of 200 μl dimethyl sulfoxide. The absorbance value was measured in a microplate reader (Bio-Rad Laboratories) at 490 nm. Values were expressed as a percentage relative to those obtained in controls.

Immunocytochemistry

Microglial cells were seeded onto glass coverslips. Following treatment with or without PA, LPS or inhibitors at the indicated times, cells were fixed in 4 % paraformaldehyde for 10 min, and blocked with 10 % goat serum in PBS. Slides were incubated overnight in a humid chamber at 4°C with the primary Ab (mouse monoclonal anti-CD11b Ab (1:100 dilution); rabbit polyclonal anti-inducible NO synthase (iNOS) Ab (1:100 dilution); rabbit monoclonal anti-NF-κB p65 Ab (1:100 dilution); all Cell Signaling Technology, Beverly, MA, USA). After primary Ab incubation, samples were washed again and incubated in the appropriate fluorescent-conjugated secondary Ab (goat anti-mouse/rabbit IgG (1:100 dilution); Sigma-Aldrich) for 1 h. The cells were counterstained by 4′,6-diamidino-2-phenylindole (DAPI). Images were captured with a Nikon TE2000U microscope.

Reverse transcription-PCR

Total RNA was extracted from induced cell cultures using the Trizol reagent (Gibco, Invitrogen Corp.) according to the manufacturer's instructions. RNA concentration was determined by a spectrophotometer (Bio-Rad Laboratories) at 260 nm. Identical amounts of RNA (1 μg) were reverse transcribed into cDNA by using a commercial RT-PCR kit (Fermentas, Vilnius, Lithuania) according to the manufacturer's instructions. cDNA was subsequently amplified by PCR with specific primers (Table 1). PCR amplification of the resulting cDNA template was conducted by using the following conditions for thirty-two (TNF-α, IL-6, iNOS and β-actin) and thirty-five (IL-1β) cycles; denaturation at 94°C for 30 s, annealing at

Table 1. PCR primers used in the present study

Gene	Forward	Reverse
TNF-α	5′-CGTCAGCCGATTTGCTATCT-3′	5′-CGGACTCCGCAAAGTCTAAG-3′
IL-1β	5′-AAGATGAAGGGCTGCTTCCAA ACC-3′	5′-ATACTGCCTGCCTGAAGCTCTTGT-3′
IL-6	5′-CCACTTCACAAGTCGGAGGCTT-3′	5′-CCAGCTTATCTGTTAGGAGA-3′
iNOS	5′-CCTCCTCCACCCTACCAAGT-3′	5′-CACCCAAAGTGCTTCAGTCA-3′
β-Actin	5′-GTGGGGCGCCCCAGGCACCA-3′	5′-CTTCCTTAATGTCACGCACGATTTC-3′

iNOS, inducible NO synthase.

60°C for 45 s, and extension at 72°C for 30 s. PCR products separated on a 1·2 % agarose–Tris-acetate-EDTA (TAE) gel were visualised by staining with ethidium bromide. The densitometric analysis of the data was normalised to β-actin. The intensity of bands was determined using the Image-Pro Plus 6.0 software (Media Cybernetics, Inc., Bethesda, MD, USA).

Western blot analysis

Cell-associated proteins were washed with cold PBS and lysed in ice-cold radioimmunoprecipitation assay (RIPA) buffer containing protein inhibitors. Cell lysates were incubated at 4°C for 20 min. The sample was centrifuged at 12 000 rpm for 10 min at 4°C, the supernatant fraction was then collected and protein concentration was assayed colorimetrically. A quantity of 30 μg total proteins was loaded onto a 4–20 % gradient polyacrylamide gel, electrophoretically transferred to a polyvinylidene difluoride membrane and probed with primary antibodies (rabbit polyclonal anti-phospho-NF-κB p65 (S536) Ab (1:500 dilution), Bioworld Technology, Inc., Minneapolis, MN, USA; rabbit monoclonal anti-NF-κB p65 Ab (1:1000 dilution), Cell Signaling Technology; rabbit polyclonal anti-iNOS Ab (1:1000 dilution), Cell Signaling Technology). Mouse monoclonal anti-β-actin (1:2000 dilution; Sigma-Aldrich) was used as an internal control. Secondary antibodies were horseradish peroxidase conjugated to goat/mouse anti-rabbit IgG (1:5000 dilution; Sigma-Aldrich). The membranes were developed using an enhanced chemiluminescence detection system (Pierce, Rockford, IL, USA).

Transient transfection and luciferase reporter gene assay

The NF-κB reporter plasmid contained three copies of the NF-κB-binding sequence fused to the firefly luciferase gene (Clontech Laboratories, Inc., Mountain View, CA, USA). The cells were cultured in a twenty-four-well plate until they reached 75–80 % confluency. Transfection of the NF-κB reporter gene into the cells was performed using Lipofectamine 2000 (Invitrogen Corp.) according to the manufacturer's instructions. Cells were transfected with 0·8 μg NF-κB reporter plasmid, 0·04 μg pRL-TK vector (Promega Corp., Madison, WI, USA) mixed with Lipofectamine 2000. After 48 h, cells were harvested and a luciferase assay was performed. To determine SFA-induced NF-κB activity, cells were incubated with or without PA or LPS for 24 h before harvesting cells for the luciferase assay. Luciferase assays were performed using the Dual-Luciferase reporter assay system (Promega Corp.) according to the manufacturer's instructions. Luciferase activity was measured using a Monolight 2010 luminometer (Analytical Luminescence Laboratory, San Diego, CA, USA). Renilla luciferase activity was used as an internal control. The relative luciferase activity was then calculated by normalising firefly luciferase activity to Renilla luciferase activity.

Statistical analysis

Quantitative data are presented as the mean values and standard deviations of at least three independent experiments. Statistical analysis of data was done by Student's *t* test or by one-way ANOVA using Dunnett's test in multiple comparisons of means. Differences were considered statistically significant if the *P* value was < 0.05.

Results

Treatment with SFA led to activation of microglial cells

In order to confirm that incubation with SFA would not induce microglia death, cell viability was assessed at 48 h after PA treatment by MTT. BV-2 cell viability following treatment with PA at 25 μM (94·78 (SD 4·34) %), 50 μM (101·09 (SD 14·61) %) and 100 μM (89·49 (SD 6·51) %) was not significantly different from the control (100·08 (SD 5) %). However, exposure of BV-2 cells to PA at 200 μM resulted in significantly fewer viable cells (66·82 (SD 4·91) %) as compared with cells in the control condition (Fig. 1(a)). In view of this and because PA is common in the diet and constitutes a large proportion of circulating NEFA, we used PA (25, 50 and 100 μM) as a representative SFA in most of the subsequent experiments.

The MTT assay showed that PA did not have any cytotoxicity at the concentrations of 25, 50 and 100 μM for at least 48 h on primary microglia (Fig. 1(a)); it was clearly toxic to cells at the concentration of 200 μM.

It is interesting to note that primary microglia were activated following treatment with PA for 6 and 24 h. This was manifested by light microscopic imaging which showed that after 6 and 24 h incubation with PA (100 μM), cells assumed a round outline or appeared amoeboid in form compared with the control cells treated with BSA and vehicle which were mostly ramified with numerous, long extending processes; very few amoeboid cells were observed in the control condition (Fig. 1(b)). Moreover, BV-2 cells treated with LPS (500 ng/ml) for 6 and 24 h also showed an activated morphology (data not shown).

Microglial activation is associated with a marked increase in CD11b expression[20]. At 24 h after treatment with PA

(100 μM), or LPS (500 ng/ml), the present results showed that there was dramatically increased CD11b expression in primary microglial cells (Fig. 1(c)).

SFA induced expression and secretion of pro-inflammatory cytokines

RT-PCR analysis showed that in BV-2 cells exposed to different concentrations of PA (25, 50 and 100 μM) or LPS (500 ng/ml) for 4 h, the levels of TNF-α, IL-1β and IL-6 mRNA expression were significantly increased compared with the control (Fig. 2(a) and (b)). By ELISA, we then determined the production of TNF-α, IL-1β and IL-6 in the medium of BV-2 cells treated with PA at different concentrations (25, 50 and 100 μM) for 12, 24 and 48 h. As a positive control, BV-2
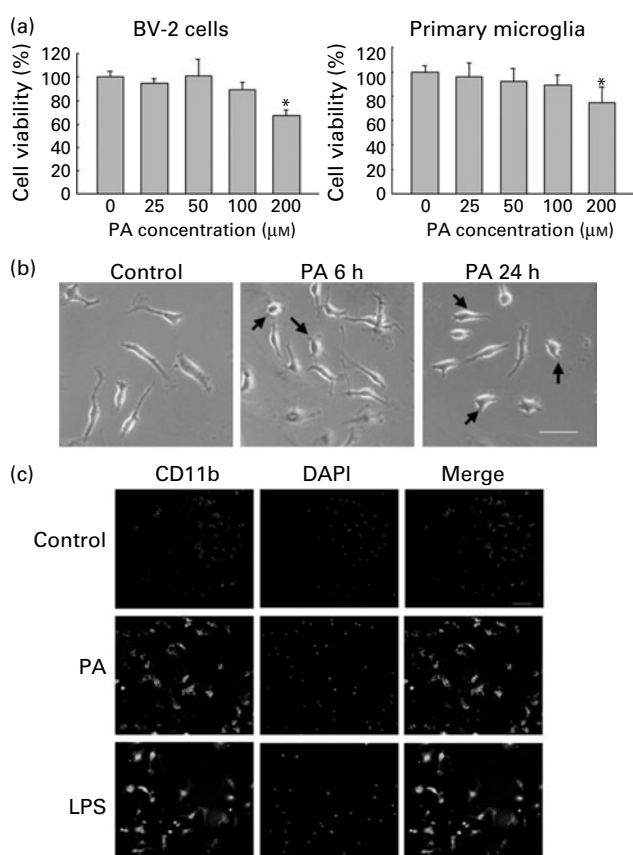
Fig. 1. Effects of SFA treatment on microglia. (a) BV-2 cells and primary microglial cells maintained in serum-free medium were incubated in the absence or presence of indicated concentrations of palmitic acid (PA; 25–200 μM) for 48 h and cell viability was performed by the 3-[4, 5-dimethylthiazol-2-yl]-2, 5-diphenyltetrazolium bromide (MTT) assay. Three independent experiments were conducted. Values are the means of three independent experiments, with standard deviations represented by vertical bars. * Mean value was significantly different from that of the control (P< 0·05). (b) Primary microglial cells were incubated in the absence or presence of PA (100 μM) for 6 and 24 h, then microscopic images were taken. Scale bar = 50 μm. Images are representative of triplicate sets. → , Primary microglial cells with a round outline or amoeboid in form. (c) Primary microglial cells were incubated in the absence or presence of PA (100 μM) or lipopolysaccharide (LPS; 500 ng/ml) for 24 h, then stained with anti-CD11b, and counterstained with 4′,6-diamidino-2-phenylindole (DAPI). Scale bar = 100 μm. Images are representative of triplicate sets.
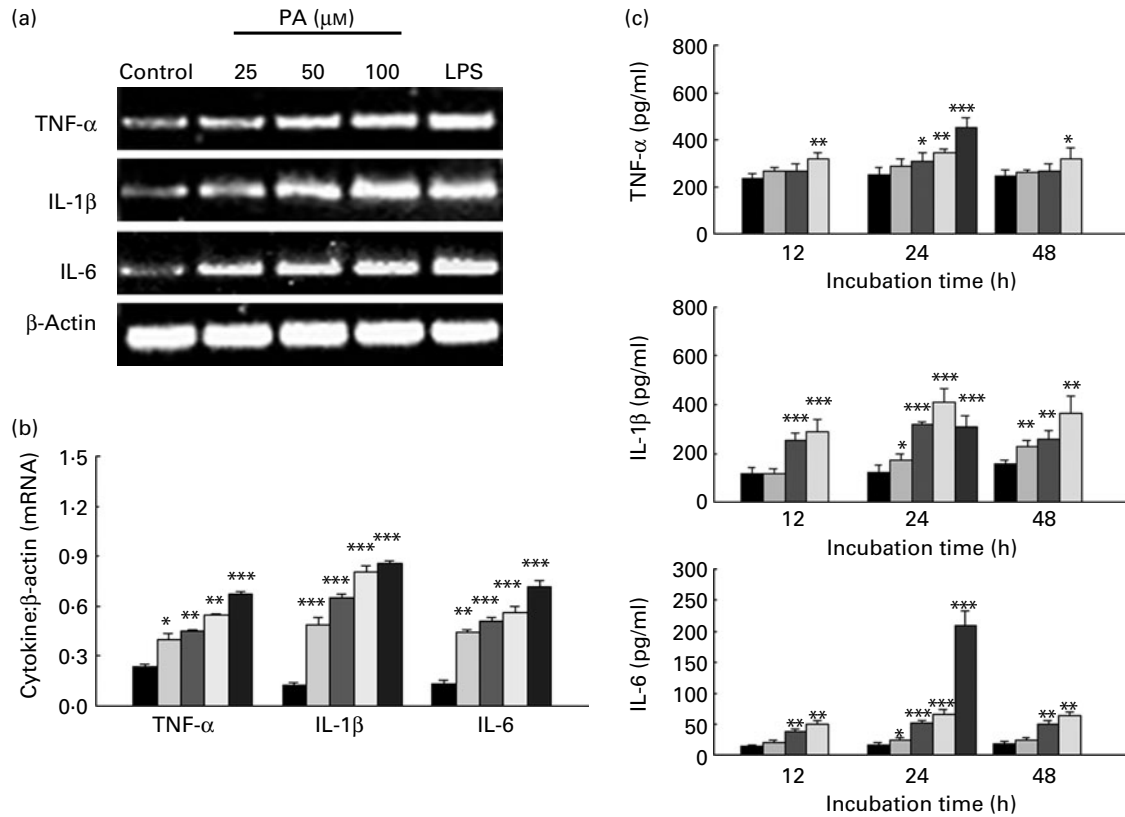
cells were stimulated with LPS (500 ng/ml) for 24 h. As shown in Fig. 2(c), both LPS and PA, at either low or high concentrations, stimulated microglia to produce increased amounts of cytokines. In addition, PA stimulated the release of TNF-α, IL-1β and IL-6 in BV-2 cells from 12 h onward at all the concentrations (25, 50 and 100 μM); the maximum production was observed at 24 h. Remarkably, IL-1β secretion of the PA-treated microglia (409·47 (SD 54·54) pg/ml) was higher than that in LPS-treated cells (306·93 (SD 45·10) pg/ml) (Fig. 2(c)) at 24 h. Nonetheless, the levels of TNF-α and IL-6 were about 1- to 2-fold higher in LPS (TNF-α, 451·14 (SD 40·95) pg/ml; IL-6, 209·88 (SD 22·60) pg/ml) than those in the PA-treated microglia (TNF-α, 344·06 (SD 18·38) pg/ml; IL-6, 65·19 (SD 8·49) pg/ml) at 24 h.

SFA caused increased NO release and intracellular inducible NO synthase levels

We first tested the effect of PA on NO release by measuring nitrite quantities in the supernatant fractions of BV-2 cell culture. It was found that upon treatment with different concentrations of PA (25, 50 and 100 μM) for 12, 24 and 48 h or LPS (500 ng/ml) for 24 h, NO release was significantly increased from the cells in all three treatment groups in a dose-dependent and time-dependent manner compared with the control (Fig. 3(a)). The cells exposed to different concentrations of PA (25, 50 and 100 μM) for 4 h also exhibited an increase in iNOS mRNA expression in a dose-dependent manner (Fig. 3(b) and (c)).

In conjunction with nitrite quantification, iNOS expression responsible for NO production was evaluated by Western blot and immunocytochemistry. Western blot results showed that PA dose-dependently increased iNOS expression in BV-2 cells (Fig. 3(c)). Moreover, in the PA (100 μM)-treated group, iNOS expression was higher than that in LPS-treated cells. By immunofluorescence, iNOS expression was induced after 6 h of treatment with PA (100 μM) in primary microglia cells; at 24 h after treatment, the expression was visibly more intense (Fig. 3(d)). In order to investigate whether the above effects are PA specific, we then tested another SFA – SA, which is present in the serum, accounting for close to 13 % of the total fatty acids. We found that treatment with 100 μM-SA (a non-toxic concentration) for 4 h also induced a marked morphological change (data not shown) and increased expression of pro-inflammatory cytokine mRNA and iNOS mRNA in BV-2 cells (Fig. 3(e)). These results suggest that SFA play a rather general role in microglial activation.

SFA caused elevation of reactive oxygen species production

We next examined whether SFA treatment could affect intracellular ROS levels in BV-2 cells. The cells were treated with PA (100 μM) for 12 and 24 h, or LPS (500 ng/ml) for 24 h, following the addition of the ROS fluorescent probes H₂DCFDA and DHE to detect H_2O_2 and superoxide ($O_2^{·-}$) production, respectively (Fig. 4(a)). It was observed that both PA

Fig. 2. SFA increase pro-inflammatory cytokine mRNA expression and secretion. (a) BV-2 cells cultured in triplicate were incubated in the absence or presence of palmitic acid (PA; 25–100 μM) or lipopolysaccharide (LPS; 500 ng/ml) for 4 h. The relative expression levels of TNF-α, IL-1β and IL-6 genes were analysed by semi-quantitative RT-PCR. Each value was normalised to β-actin. (b) Quantification of mRNA levels of the various cytokines determined by Image-Pro Plus 6·0. (c) BV-2 cells cultured in triplicate were incubated in the absence or presence of PA (25–100 μM) for 12, 24 and 48 h or LPS (500 ng/ml) for 24 h. The levels of pro-inflammatory cytokines were measured by ELISA. (■), Control; (▨), 25 μM-PA; (■), 50 μM-PA; (□), 100 μM-PA; (■), LPS. Values are the means of three independent experiments, with standard deviations represented by vertical bars. Mean value was significantly different from that of the control: * $P<0.05$, ** $P<0.01$, *** $P<0.001$.

and LPS markedly increased H_2O_2 and O_2^- production in BV-2 cells compared with the control (Fig. 4(b)).

Activation of microglia by palmitic acid treatment leads to bystander neuronal death

Activated microglia are known to produce an array of cytokines and other inflammatory mediators that are in turn deleterious for surrounding neurons in the CNS[21]. BV-2 cells were incubated in the absence or presence of PA (25, 50 and 100 μM) for 12 h and the medium was changed with fresh serum-free DMEM. After 12 h, supernatant fractions were collected and filtered. To check whether PA-induced microglia activation causes bystander neuronal death, we treated primary neurons with the medium mentioned above. The control comprised culture supernatant fractions from BSA- and vehicle-treated BV-2 cells. Primary cortical neurons were incubated with microglia-conditioned medium for 2 d and then neuronal apoptosis was measured by morphological analysis. The results in Fig. 5 demonstrated a significant induction of apoptosis in the neurons. These results indicate that microglia produced inflammatory mediators in response to PA and that the mediators accumulated in the medium were capable of inducing neuronal death.

SFA-activated NF-κB signalling

NF-κB is an essential transcription factor for the expression of cytokine and iNOS expression in microglia[22]. We therefore investigated the potential nuclear translocation of NF-κB following the stimulation of microglia with PA. For these experiments, BV-2 cells were treated with or without PA (100 μM) or LPS (500 ng/ml) for 1 h, and the p65 subunit of NF-κB in the nuclear fraction was assessed by using immunofluorescence. It was observed that either PA or LPS was capable of activating NF-κB, as demonstrated by the increased levels of the NF-κB subunit, p65, in the nucleus, whereas p65 was localised primarily in the cytosol during the resting state (Fig. 6(a)).

It has been demonstrated that phosphorylation of serine residues 529 and 536 of the RelA/p65 subunit leads to a transactivation of NF-κB[23]. We next investigated whether PA regulates the phosphorylation of p65. The proteins harvested from the cells after 1 h treatment with or without PA (25, 50 and 100 μM) were processed for Western blot to detect intracellular levels of phospho-p65 (ser536). As shown in Fig. 6(b), phospho-p65 levels were significantly elevated in all three treatment groups.

In order to observe the effect of PA on the transcriptional activity of NF-κB, cells were transfected with a plasmid construct containing 3 × NF-κB binding sites associated with the
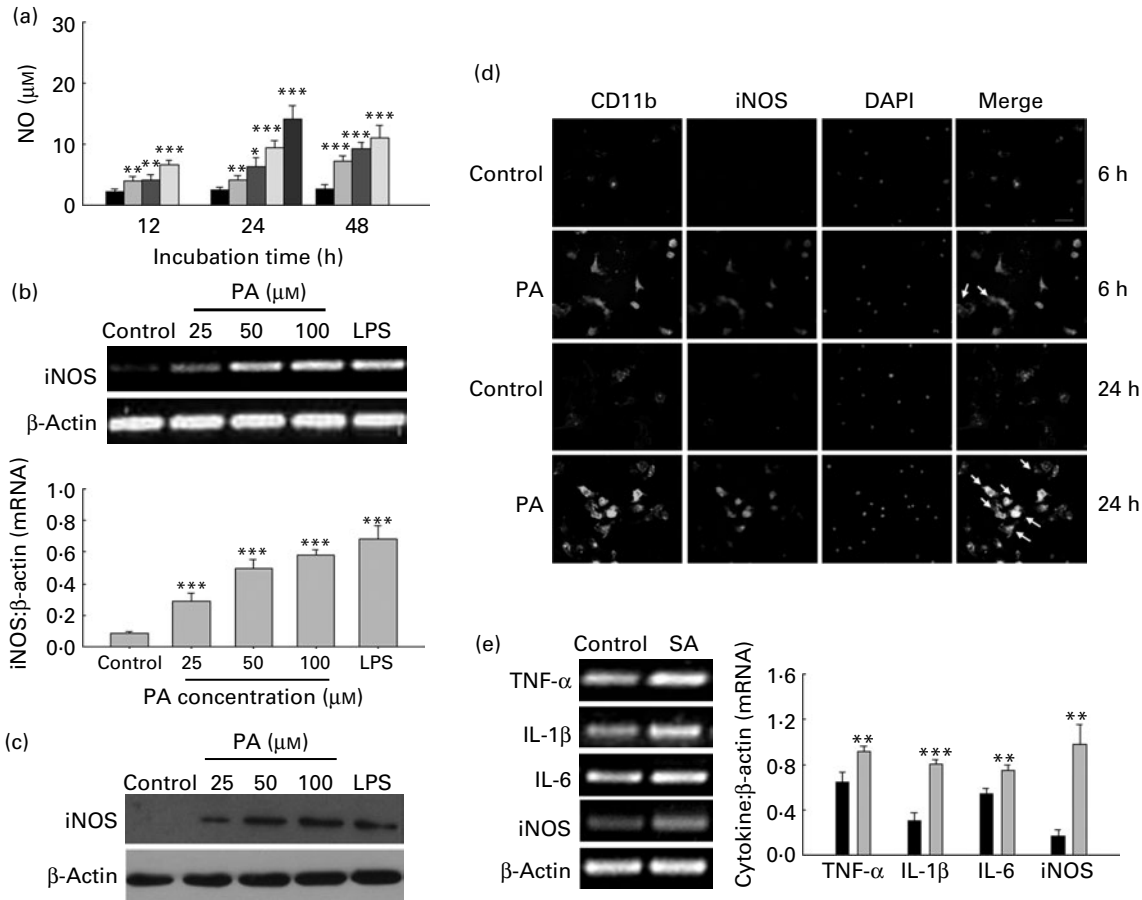
Fig. 3. SFA cause elevated NO release from BV-2 cells and increase inducible NO synthase (iNOS) expression. (a) NO was determined by Greiss reagent after BV-2 cells cultured in triplicate were incubated in the absence or presence of palmitic acid (PA; 25–100 μM) for 12, 24 and 48 h, or lipopolysaccharide (LPS; 500 ng/ml) for 24 h. (■), Control; (□), 25 μM-PA; (■), 50 μM-PA; (□), 100 μM-PA; (■), LPS. (b) BV-2 cells were incubated in the absence or presence of PA (25–100 μM) or LPS (500 ng/ml) for 4 h. The relative expression level of the iNOS gene was analysed by semi-quantitative RT-PCR. Each value was normalised to β-actin. Quantification of the mRNA levels of iNOS determined by Image-Pro Plus 6·0. (c) BV-2 cells were incubated in the absence or presence of PA (25–100 μM) or LPS (500 ng/ml) for 24 h and 30 μg of total protein were subjected to Western blot analysis. (d) Following treatment with or without PA (100 μM) for 6 h and 24 h, primary microglial cells were stained with anti-CD11b, anti-iNOS and counterstained with 4′,6-diamidino-2-phenylindole (DAPI). Scale bar = 50 μm. (e) BV-2 cells were incubated in the absence (■) or presence (□) of stearic acid (SA; 100 μM) for 4 h. The relative expression levels of TNF-α, IL-1β, IL-6 and iNOS genes were analysed by semi-quantitative RT-PCR. Quantification of mRNA determined by Image-Pro Plus 6·0. Images are representative of triplicate sets. Values are the means of three independent experiments, with standard deviations represented by vertical bars. Mean value was significantly different from that of the control: **$P < 0.01$, ***$P < 0.001$.

luciferase reporter plasmid and a control vector. It was observed that PA (25, 50 and 100 μM) exposure induced NF-κB-driven luciferase activity in a dose-dependent manner (Fig. 6(c)).

NF-κB inhibitor suppressed SFA-induced pro-inflammatory cytokines and NO production

The role of NF-κB in PA-induced pro-inflammatory cytokines and NO production was examined using the specific NF-κB pathway inhibitor PDTC. In BV-2 cells treated with PDTC (100 μM, a non-toxic concentration), for 4 h, PA-induced gene expression of iNOS and pro-inflammatory cytokines was significantly suppressed (Fig. 7(a) and (b)). In addition, PDTC reduced PA-induced NO, TNF-α and IL-1β secretion (Fig. 7(c)). However, PDTC did not exert a significant effect on PA-induced IL-6 production (Fig. 7(c)). Taken together with the result shown in Fig. 6, these findings indicate that

SFA are capable of inducing a rapid response of NF-κB in microglia, triggering the expression of cytokines (for example, TNF-α and IL-1β) and inflammatory mediators such as NO.

Anti-Toll-like receptor 4 antibody inhibited SFA-induced NF-κB activation and pro-inflammatory mediator production

We next investigated whether PA-induced activation of NF-κB was regulated via TLR4. Fig. 8(a) shows that at 1 h of PA treatment, the p65 translocation of NF-κB was significantly increased. Incubating the cells with anti-TLR4 Ab (10 μg/ml, a non-toxic concentration), however, prevented the PA-induced activation of NF-κB, suggesting an involvement of TLR4 in the activation of the transcriptional factors. Moreover, treatment of BV-2 cells with anti-TLR4 Ab inhibited PA-induced production of pro-inflammatory mediators (Fig. 8(b)).
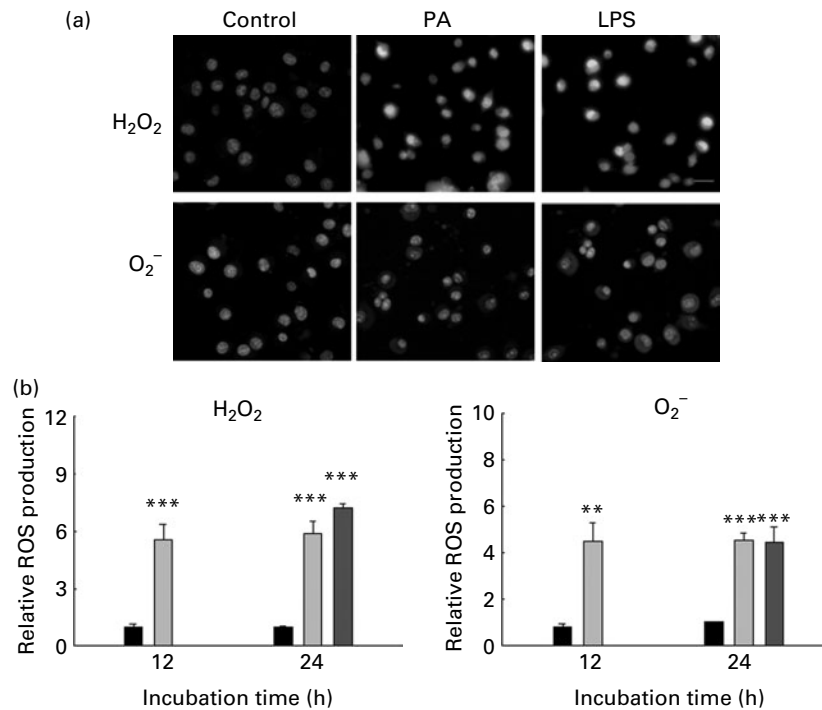
Fig. 4. SFA increase intracellular reactive oxygen species (ROS). (a) BV-2 cells were incubated in the absence or presence of palmitic acid (PA; 100 μM) for 12 and 24 h, or lipopolysaccharide (LPS; 500 ng/ml) for 24 h. Following incubation and washing with PBS, the cells were treated with 10 μM-2',7'-dichlorodihydrofluor-escein diacetate (H_2DCFDA) or 2 μM-dihydroethidium (DHE) and counterstained with 4',6-diamidino-2-phenylindole (DAPI), and ROS were detected by using a flu-orescence microscope. Scale bar = 20 μm. Images are representative of triplicate sets. (b) Quantification of the ROS was determined by fluorescence plate reader. (■), Control; (□), PA; (■), LPS. Values are the means of four independent experiments, with standard deviations represented by vertical bars. Mean value was significantly different from that of the control: ** $P < 0.01$, *** $P < 0.001$.

Discussion

The present results have shown that SFA can induce microglial activation as manifested by its actions on BV-2 cells and primary microglial cells. We have shown that SFA treatment induced microglial activation, as shown by changes in cell morphology consistent with a reactive phenotype, and caused significantly higher production of ROS, NO, and pro-inflammatory cytokines including TNF-α, IL-1β and IL-6 in microglia, resulting in bystander neuronal death. Moreover, PA treatment induced a marked expression of IL-1β and iNOS comparable with that with LPS. Additionally, we have shown that PA treatment activated NF-κB. It is striking that inhibition of NF-κB activation, with its inhibitor PDTC resulted in inhibition of iNOS, TNF-α, IL-1β and IL-6 mRNA expression, and production of TNF-α, IL-1β and NO except for IL-6. Another major finding was that in cells treated with anti-TLR4 Ab, PA-induced NF-κB activation and pro-inflammatory mediator production were repressed. These results suggest that SFA could activate microglia and stimulate the TLR4–NF-κB pathway to trigger the production of pro-inflammatory mediators, which may contribute to neuronal death.

Microglia adapt to different CNS environments and exhibit diverse morphological types and functional specialisations[24]. Our findings have demonstrated that BV-2 cells and primary microglial cells exposed to SFA assumed an amoeboid mor-phology and increased CD11b expression, which are indica-tive of its activated state.

It has been reported that the pro-inflammatory cytokines TNF-α, IL-1β and IL-6, which are important factors in the regu-lation of inflammatory processes, are overexpressed in the brain of AD patients[25–27], indicating the possible involve-ment of these cytokines in the pathology of the disease. Indeed, the present results have shown that PA and SA increased TNF-α, IL-1β and IL-6 mRNA expression and cyto-kine secretion. Along with the pro-inflammatory cytokines, NO is an important contributor to neuronal damage in AD development[28]. Following PA stimulation, there was a marked increase in NO production by BV-2 cells. Moreover, iNOS expression was also enhanced after PA treatment for 6 and 24 h. It is suggested that SFA treatment had induced iNOS up-regulation in microglia resulting in increased pro-duction of NO.

Like LPS, PA enhanced TNF-α, IL-6 and IL-1β production in microglia. However, it is remarkable that PA treatment had resulted in more vigorous IL-1β up-regulation. IL-1β is a criti-cal inflammatory cytokine in AD, and found in activated microglia localised to amyloid plaques[29]. IL-1β induces amy-loid β deposition through directly up-regulating expression and processing of β-amyloid precursor proteins[30,31]. It increases tau phosphorylation by mitogen-activated protein kinase p38[32]. It activates astrocytes to overexpress S100 β, which stimulates neurite growth and increases Ca flux (a deadly event) in neurons[33]. Moreover, it also stimulates astro-cytes to produce additional pro-inflammatory cytokines such as IL-6[34,35]. IL-1β has been reported to promote the
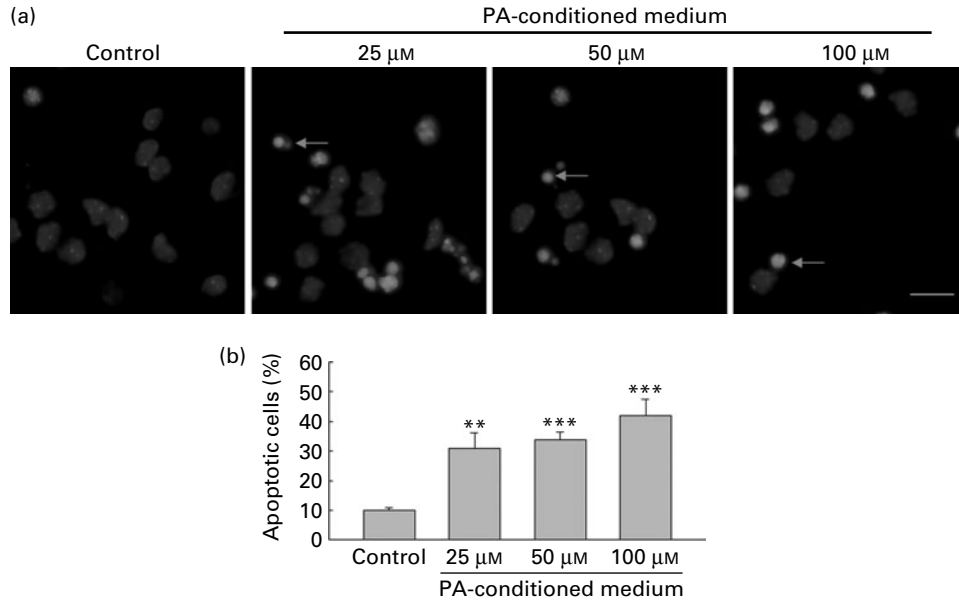
Fig. 5. Bystander neuronal death caused by SFA-treated microglia. (a) BV-2 cells were incubated in the absence or presence of palmitic acid (PA; 25–100 μM) for 12 h. The medium was changed with fresh serum-free Dulbecco's modified Eagle's medium (DMEM) for 12 h. The supernatant fractions were collected, filtered and stored at −20°C. Primary cortical neurons were treated with these culture supernatant fractions for 48 h and stained with Hoechst 33 342. ←, Representative apoptotic nuclei (scale bar = 10 μm). Images are representative of triplicate sets. (b) Apoptotic nuclei were quantified in ten random fields for each experimental condition. Values are the means of three independent experiments, with standard deviations represented by vertical bars. Mean value was significantly different from that of the control: ** $P < 0.01$, *** $P < 0.001$.

activation activity of the enzyme acetylcholinesterase, thus down-regulating the cholinergic system[36]. Finally, IL-1 directly promotes microglial proliferation[37] and increases microglial expression of IL-1β and IL-6[38]. All these IL-1β-regulated processes might result in neuronal stress or injury, which in turn further enhances microglial activation and

IL-1β overexpression. Thus IL-1β plays a pivotal role in the pathogenesis of AD. In addition, IL-1β is known to be involved in the expression and activation of iNOS[39]. Interestingly, we have found that PA treatment enhanced a marked iNOS expression at a level comparable with that induced by LPS. It is suggested that PA directly activates microglia, and
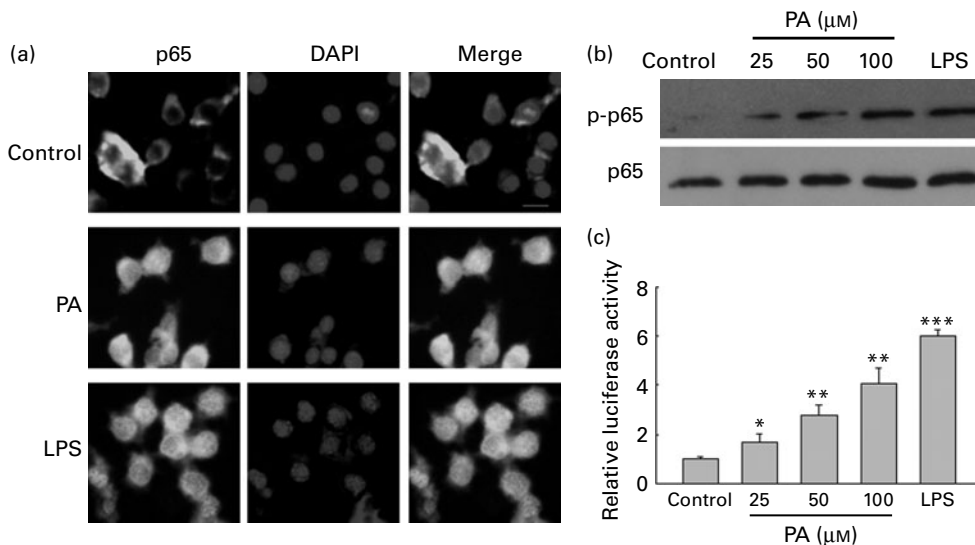

Fig. 6. SFA induce NF-κB activation. (a) BV-2 cells were incubated in the absence or presence of palmitic acid (PA; 100 μM) or lipopolysaccharide (LPS; 500 ng/ml) for 1 h and stained for NF-κB p65 and counterstained with 4′,6-diamidino-2-phenylindole (DAPI). Then images were captured by a fluorescence microscope. Scale bar = 20 μm. (b) BV-2 cells were incubated in the absence or presence of PA (25–100 μM) or LPS (500 ng/ml) for 1 h and 30 μg total protein were subjected to Western blot analysis. A phospho-specific antibody that recognises the phosphorylation of the serine 536 residue on the p65 (p-p65) determined the relative activation state of NF-κB. A non-phospho-specific antibody to NF-κB p65 (p65) served as protein loading controls. Images are representative of triplicate sets. (c) BV-2 cells were incubated in the absence or presence of PA (25–100 μM) or LPS (500 ng/ml) for 24 h. The effect of PA on NF-κB promoter activity was evaluated by luciferase assay as described in Materials and methods. Values are the means of three independent experiments, with standard deviations represented by vertical bars. Mean value was significantly different from that of the control: * $P < 0.05$, ** $P < 0.01$, *** $P < 0.001$.
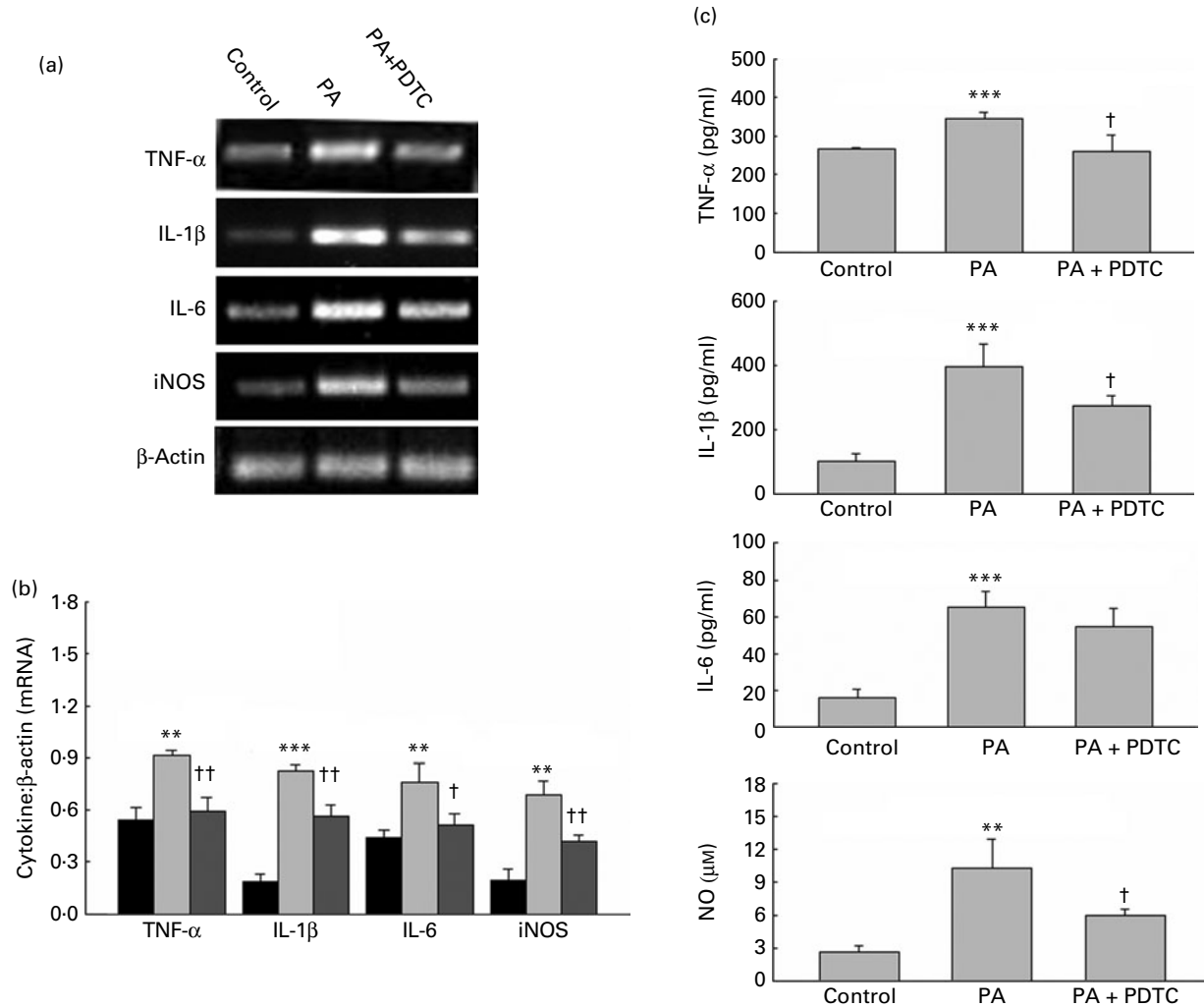
Fig. 7. Pyrrolidine dithiocarbamate (PDTC) inhibits SFA-induced cytokine and NO release. (a) BV-2 cells were incubated in the absence or presence of palmitic acid (PA; 100 μM), alone or in combination with PDTC (100 μM), for 4 h. The relative expression levels of TNF-α, IL-1β, IL-6 and inducible NO synthase (iNOS) genes were analysed by semi-quantitative RT-PCR. Each value was normalised to β-actin. (b) Quantification of mRNA levels of TNF-α, IL-1β, IL-6 and iNOS determined by Image-Pro Plus 6·0. (■), Control; (□), PA; (■), PA + PDTC. (c) BV-2 cells were incubated in the absence or presence of PA (100 μM), alone and in combination with PDTC (100 μM), for 24 h. TNF-α, IL-1β, IL-6 and NO production was measured. Values are the means of four independent experiments, with standard deviations represented by vertical bars. Mean value was significantly different from that of the control: ** $P < 0.01$, *** $P < 0.001$. Mean value was significantly different from that of PA alone: † $P < 0.05$, †† $P < 0.01$.

increases IL-1β production, which may lead to enhanced iNOS expression. The above results indicate that IL-1β may play a key and detrimental role in regulating the SFA-induced inflammatory response.

Analysis of the regulation of inducible transcription factors has claimed a major role for the NF-κB system in the activation of microglial cells in neurodegenerative diseases. Activation of NF-κB has been linked to the up-regulation of potentially inflammation-related genes, including iNOS, cyclo-oxygenase-2, TNF-α, IL-1β and IL-6. Previous studies have demonstrated that SFA can induce NF-κB activation in macrophages[40]. The present results have shown that PA enhanced p65 nuclear translocation, phosphorylation and NF-κB promoter activity. Furthermore, PDTC, a potent NF-κB inhibitor, suppressed PA-induced NO, TNF-α and IL-1β production in BV-2 cells, while PA-induced IL-6 production was not affected. It is therefore suggested that NO, TNF-α and IL-1β are downstream gene products of the NF-κB pathway induced by PA, whereas the effect of PA on IL-6 is independent of the NF-κB pathway. It is possible that other transcriptional factors may be involved in IL-6 production, for example, activating protein-1[41], cAMP-induced transcription factors such as cAMP-responsive element binding protein and CCAAT-enhancer box binding protein[42,43], or signal transducer and activator of transcription[44]. PA may be able to activate one of these transcriptional factors, increasing IL-6 production.

Several previous results have demonstrated that the stimulation of TLR4 by SFA can trigger transcription factor activation, leading to the production of pro-inflammatory mediators in monocytes and macrophages *in vitro*[45]. However, recent studies have called into question the ability of
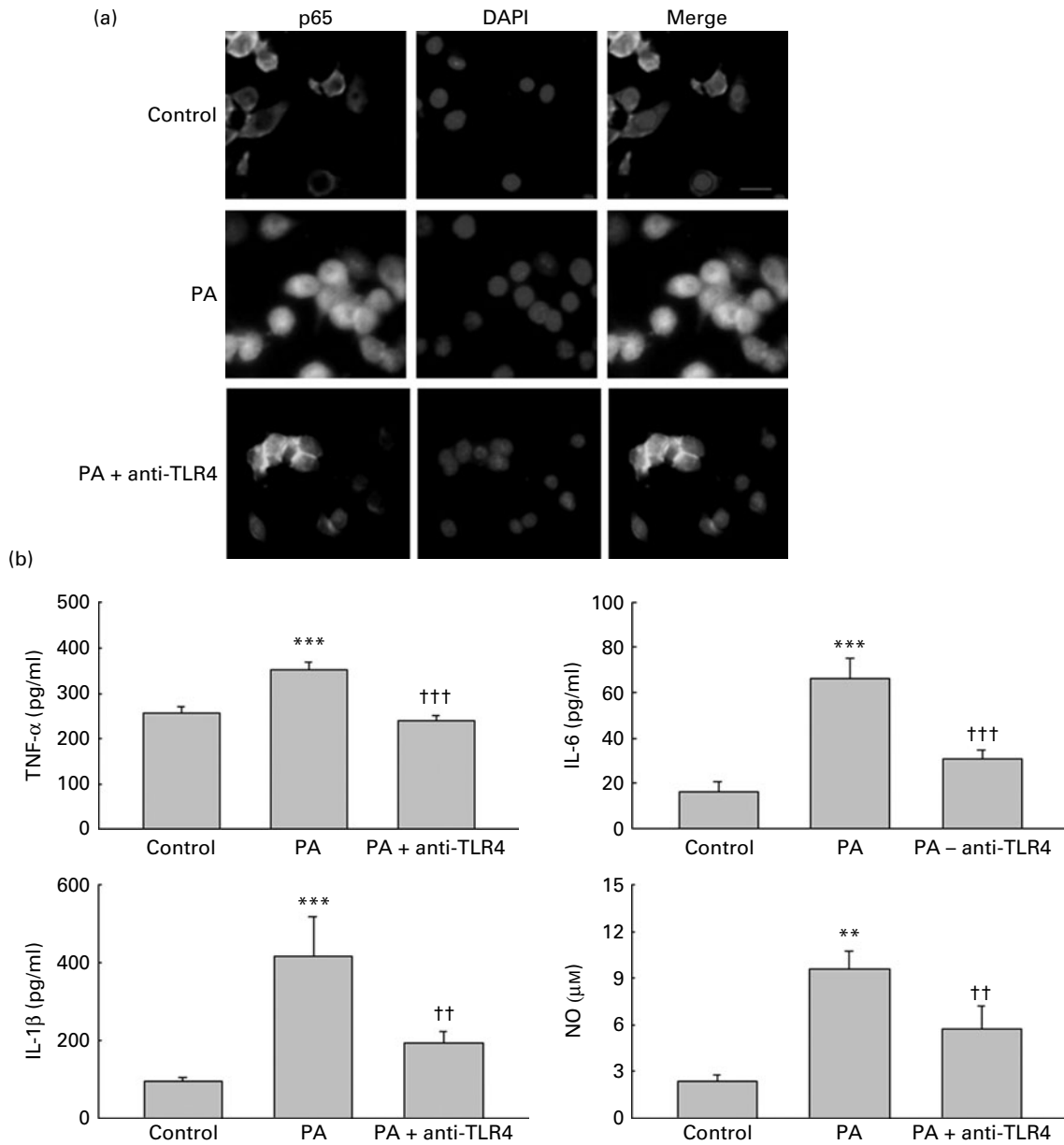
Fig. 8. Effects of antibody-mediated Toll-like receptor (TLR)-4 blockade on SFA-induced NF-κB activation and pro-inflammatory mediator production. (a) BV-2 cells were incubated in the absence or presence of PA (100 μM), alone or in combination with anti-TLR4-neutralising antibody for 1 h. The cells were stained for NF-κB p65 and counterstained with 4′,6-diamidino-2-phenylindole (DAPI). Then images were captured in a fluorescence microscope. Scale bar = 20 μm. Images are representative of triplicate sets. (b) BV-2 cells were incubated in the absence or presence of PA (100 μM), alone and in combination with anti-TLR4-neutralising antibody for 24 h. TNF-α, IL-1β, IL-6 and NO production was measured. Values are the means of four independent experiments, with standard deviations represented by vertical bars. Mean value was significantly different from that of the control: ** $P < 0.01$, *** $P < 0.001$. Mean value was significantly different from that of PA alone: †† $P < 0.01$, ††† $P < 0.001$.

TLR to directly bind SFA as a ligand and suggest that SFA might modulate TLR activity via lipid raft changes[46] or that SFA may induce inflammation via TLR-independent mechanisms[47]. In the present study anti-TLR4 Ab reversed the PA-induced NF-κB p65 translocation and pro-inflammatory mediator production. Thus, it is hypothesised that TLR4 may mediate NF-κB activation in PA-induced microglia activation. On the other hand, the mechanism by which PA can activate TLR4 remains to be clarified. It is evident that the above-mentioned effects of SFA on BV-2 cells were not due to cytotoxicity, because no significant cell death was observed in the concentration ranges examined.

Against the above background, we then determined whether culture supernatant fractions derived from microglia treated with PA could actually affect neuronal survivability. Indeed, on addition of the supernatant fractions into primary neuronal culture, there was a significant reduction of neuronal viability. Thus, the combination of ROS, NO and pro-inflammatory cytokines seems to act in a synergistic way to cause bystander death to neurons.

In conclusion, the present study has shown that SFA can cause activation of microglial cells, resulting in the generation of pro-inflammatory cytokines, NO and ROS, which could, in turn, induce neuronal dysfunctions. PA treatment markedly increases the expression of IL-1β and iNOS to a level comparable with that with LPS. PA induced the TLR4-mediated activation of NF-κB, which is responsible for TNF-α, IL-1β and NO production. The possibility of PA activation of other pathways should be considered. This takes into consideration the fact that inhibition of NF-κB did not alter IL-6 production. The present novel findings suggest the potential mechanisms in SFA-induced microglial activation and, to this end, nutrition rich in SFA may be linked to some inflammatory diseases of the CNS.

Acknowledgements

References

1. Eskelinen MH, Ngandu T, Helkala EL, *et al.* (2008) Fat intake at midlife and cognitive impairment later in life: a population-based CAIDE study. *Int J Geriatr Psychiatry* **23**, 741–747.

2. Morris MC, Evans DA, Bienias JL, *et al.* (2004) Dietary fat intake and 6-year cognitive change in an older biracial community population. *Neurology* **62**, 1573–1579.

3. Solfrizzi V, D'Introno A, Colacicco AM, *et al.* (2005) Dietary fatty acids intake: possible role in cognitive decline and dementia. *Exp Gerontol* **40**, 257–270.

4. Morris MC, Evans DA, Tangney CC, *et al.* (2006) Dietary copper and high saturated and *trans* fat intakes associated with cognitive decline. *Arch Neurol* **63**, 1085–1088.

5. Greenwood CE & Winocur G (1996) Cognitive impairment in rats fed high-fat diets: a specific effect of saturated fatty-acid intake. *Behav Neurosci* **110**, 451–459.

6. Granholm AC, Bimonte-Nelson HA, Moore AB, *et al.* (2008) Effects of a saturated fat and high cholesterol diet on memory and hippocampal morphology in the middle-aged rat. *J Alzheimers Dis* **14**, 133–145.

7. Dhopeshwarkar GA & Mead JF (1973) Uptake and transport of fatty acids into the brain and the role of the blood–brain barrier system. *Adv Lipid Res* **11**, 109–142.

8. Wang SW, Wang M, Grossman BM, *et al.* (1994) Effects of dietary fat on food intake and brain uptake and oxidation of fatty acids. *Physiol Behav* **56**, 517–522.

9. Goux WJ, Rodriguez S & Sparkman DR (1995) Analysis of the core components of Alzheimer paired helical filaments. A gas chromatography/mass spectrometry characterization of fatty acids, carbohydrates and long-chain bases. *FEBS Lett* **366**, 81–85.

10. Roher AE, Weiss N, Kokjohn TA, *et al.* (2002) Increased Aβ peptides and reduced cholesterol and myelin proteins characterize white matter degeneration in Alzheimer's disease. *Biochemistry* **41**, 11080–11090.

11. Patil S & Chan C (2005) Palmitic and stearic fatty acids induce Alzheimer-like hyperphosphorylation of tau in primary rat cortical neurons. *Neurosci Lett* **384**, 288–293.

12. Patil S, Sheng L, Masserang A, *et al.* (2006) Palmitic acid-treated astrocytes induce BACE1 upregulation and accumulation of C-terminal fragment of APP in primary cortical neurons. *Neurosci Lett* **406**, 55–59.

13. Patil S, Melrose J & Chan C (2007) Involvement of astroglial ceramide in palmitic acid-induced Alzheimer-like changes in primary neurons. *Eur J Neurosci* **26**, 2131–2141.

14. Wilson DM & Binder LI (1997) Free fatty acids stimulate the polymerization of tau and amyloid β peptides. *In vitro* evidence for a common effector of pathogenesis in Alzheimer's disease. *Am J Pathol* **150**, 2181–2195.

15. Frank-Cannon TC, Alto LT, McAlpine FE, *et al.* (2009) Does neuroinflammation fan the flame in neurodegenerative diseases? *Mol Neurodegener* **4**, 47.

16. Block ML & Hong JS (2007) Chronic microglial activation and progressive dopaminergic neurotoxicity. *Biochem Soc Trans* **35**, 1127–1132.

17. Cao Q, Lu J, Kaur C, *et al.* (2008) Expression of Notch-1 receptor and its ligands Jagged-1 and Delta-1 in amoeboid microglia in postnatal rat brain and murine BV-2 cells. *Glia* **56**, 1224–1237.

18. Lee JY, Sohn KH, Rhee SH, *et al.* (2001) Saturated fatty acids, but not unsaturated fatty acids, induce the expression of cyclooxygenase-2 mediated through Toll-like receptor 4. *J Biol Chem* **276**, 16683–16689.

19. Fernandez-Lizarbe S, Pascual M & Guerri C (2009) Critical role of TLR4 response in the activation of microglia induced by ethanol. *J Immunol* **183**, 4733–4744.

20. Brahmachari S, Jana A & Pahan K (2009) Sodium benzoate, a metabolite of cinnamon and a food additive, reduces microglial and astroglial inflammatory responses. *J Immunol* **183**, 5917–5927.

21. Ghoshal A, Das S, Ghosh S, *et al.* (2007) Proinflammatory mediators released by activated microglia induces neuronal death in Japanese encephalitis. *Glia* **55**, 483–496.

22. Pahl HL (1999) Activators and target genes of Rel/NF-κB transcription factors. *Oncogene* **18**, 6853–6866.

23. Neumann M & Naumann M (2007) Beyond IκBs: alternative regulation of NF-κB activity. *FASEB J* **21**, 2642–2654.

24. Henn A, Lund S, Hedtjarn M, *et al.* (2009) The suitability of BV2 cells as alternative model system for primary microglia cultures or for animal experiments examining brain inflammation. *ALTEX* **26**, 83–94.

25. Tobinick E (2009) Tumour necrosis factor modulation for treatment of Alzheimer's disease: rationale and current evidence. *CNS Drugs* **23**, 713–725.

26. Di Bona D, Plaia A, Vasto S, *et al.* (2008) Association between the interleukin-1β polymorphisms and Alzheimer's disease: a systematic review and meta-analysis. *Brain Res Rev* **59**, 155–163.

27. Hull M, Berger M, Volk B, *et al.* (1996) Occurrence of interleukin-6 in cortical plaques of Alzheimer's disease patients may precede transformation of diffuse into neuritic plaques. *Ann N Y Acad Sci* **777**, 205–212.

28. Wei T, Chen C, Hou J, *et al.* (2000) Nitric oxide induces oxidative stress and apoptosis in neuronal cells. *Biochim Biophys Acta* **1498**, 72–79.

29. Sheng JG, Mrak RE & Griffin WS (1995) Microglial interleukin-1α expression in brain regions in Alzheimer's disease: correlation with neuritic plaque distribution. *Neuropathol Appl Neurobiol* **21**, 290–301.

30. Forloni G, Demicheli F, Giorgi S, *et al.* (1992) Expression of amyloid precursor protein mRNAs in endothelial, neuronal and glial cells: modulation by interleukin-1. *Brain Res Mol Brain Res* **16**, 128–134.

31. Goldgaber D, Harris HW, Hla T, *et al.* (1989) Interleukin 1 regulates synthesis of amyloid β-protein precursor mRNA in human endothelial cells. *Proc Natl Acad Sci U S A* **86**, 7606–7610.

32. Li Y, Liu L, Barger SW, *et al.* (2003) Interleukin-1 mediates pathological effects of microglia on tau phosphorylation and on synaptophysin synthesis in cortical neurons through a p38-MAPK pathway. *J Neurosci* **23**, 1605–1611.

33. Sheng JG, Ito K, Skinner RD, *et al.* (1996) *In vivo* and *in vitro* evidence supporting a role for the inflammatory cytokine interleukin-1 as a driving force in Alzheimer pathogenesis. *Neurobiol Aging* **17**, 761–766.

34. Blom MA, van Twillert MG, de Vries SC, *et al.* (1997) NSAIDS inhibit the IL-1 β-induced IL-6 release from human post-mortem astrocytes: the involvement of prostaglandin E2. *Brain Res* **777**, 210–218.

35. Griffin WS, Sheng JG, Royston MC, *et al.* (1998) Glial–neuronal interactions in Alzheimer's disease: the potential role of a 'cytokine cycle' in disease progression. *Brain Pathol* **8**, 65–72.

36. Li Y, Liu L, Kang J, *et al.* (2000) Neuronal–glial interactions mediated by interleukin-1 enhance neuronal acetylcholinesterase activity and mRNA expression. *J Neurosci* **20**, 149–155.

37. Ganter S, Northoff H, Mannel D, *et al.* (1992) Growth control of cultured microglia. *J Neurosci Res* **33**, 218–230.

38. Sebire G, Emilie D, Wallon C, *et al.* (1993) *In vitro* production of IL-6, IL-1β, and tumor necrosis factor α by human embryonic microglial and neural cells. *J Immunol* **150**, 1517–1523.

39. Akama KT & Van Eldik LJ (2000) β-Amyloid stimulation of inducible nitric-oxide synthase in astrocytes is interleukin-1β- and tumor necrosis factor-α (TNFα)-dependent, and involves a TNFα receptor-associated factor- and NFκB-inducing kinase-dependent signaling mechanism. *J Biol Chem* **275**, 7918–7924.

40. Shi H, Kokoeva MV, Inouye K, *et al.* (2006) TLR4 links innate immunity and fatty acid-induced insulin resistance. *J Clin Invest* **116**, 3015–3025.

41. Rohrbach S, Engelhardt S, Lohse MJ, *et al.* (2007) Activation of AP-1 contributes to the β-adrenoceptor-mediated myocardial induction of interleukin-6. *Mol Med* **13**, 605–614.

42. Spooren A, Kooijman R, Lintermans B, *et al.* (2010) Cooperation of NFκB and CREB to induce synergistic IL-6 expression in astrocytes. *Cell Signal* **22**, 871–881.

43. Tchivileva IE, Tan KS, Gambarian M, *et al.* (2009) Signaling pathways mediating β3-adrenergic receptor-induced production of interleukin-6 in adipocytes. *Mol Immunol* **46**, 2256–2266.

44. Lee C, Lim HK, Sakong J, *et al.* (2006) Janus kinase-signal transducer and activator of transcription mediates phosphatidic acid-induced interleukin (IL)-1β and IL-6 production. *Mol Pharmacol* **69**, 1041–1047.

45. Laine PS, Schwartz EA, Wang Y, *et al.* (2007) Palmitic acid induces IP-10 expression in human macrophages via NF-κB activation. *Biochem Biophys Res Commun* **358**, 150–155.

46. Wong SW, Kwon MJ, Choi AM, *et al.* (2009) Fatty acids modulate Toll-like receptor 4 activation through regulation of receptor dimerization and recruitment into lipid rafts in a reactive oxygen species-dependent manner. *J Biol Chem* **284**, 27384–27392.

47. Erridge C & Samani NJ (2009) Saturated fatty acids do not directly stimulate Toll-like receptor signaling. *Arterioscler Thromb Vasc Biol* **29**, 1944–1949.